Defining the Stressome of *Mycobacterium avium* subsp. *paratuberculosis* In Vitro and in Naturally Infected Cows[▽][†]

Chia-wei Wu, Shelly K. Schmoller, Sung Jae Shin,[‡] and Adel M. Talaat*

*Laboratory of Bacterial Genomics, Department of Pathobiological Sciences, University of Wisconsin—Madison,
1656 Linden Drive, Madison, Wisconsin 53706*

Mycobacterium avium **subsp.** *paratuberculosis* **causes an enteric infection in cattle, with a great impact on the dairy industry in the United States and worldwide. Characterizing the gene expression profile of *M. avium* subsp.** *paratuberculosis* **exposed to different stress conditions, or shed in cow feces, could improve our understanding of the pathogenesis of *M. avium* subsp.** *paratuberculosis***. In this report, the stress response of *M. avium* subsp.** *paratuberculosis* **on a genome-wide level (stressome) was defined for the first time using DNA microarrays. Expression data analysis revealed unique gene groups of *M. avium* subsp.** *paratuberculosis* **that were regulated under in vitro stressors while additional groups were regulated in the cow samples. Interestingly, acidic pH induced the regulation of a large number of genes ($n = 597$), suggesting the high sensitivity of *M. avium* subsp.** *paratuberculosis* **to acidic environments. Generally, responses to heat shock, acidity, and oxidative stress were similar in *M. avium* subsp.** *paratuberculosis* **and *Mycobacterium tuberculosis*, suggesting common pathways for mycobacterial defense against stressors. Several sigma factors (e.g.,** *sigH* **and** *sigE***) were differentially coregulated with a large number of genes depending on the type of each stressor. Subsequently, we analyzed the virulence of six *M. avium* subsp.** *paratuberculosis* **mutants with inactivation of differentially regulated genes using a murine model of paratuberculosis. Both bacterial and histopathological examinations indicated the attenuation of all gene mutants, especially those selected based on their expression in the cow samples (e.g.,** *lipN***). Overall, the employed approach profiled mycobacterial genetic networks triggered by variable stressors and identified a novel set of putative virulence genes. A similar approach could be applied to analyze other intracellular pathogens.**

Mycobacterium avium subsp. *paratuberculosis* is the causative agent of Johne's disease in cattle (10) and might be implicated in Crohn's disease in humans (27, 28). Infection with *M. avium* subsp. *paratuberculosis* results in a chronic infection of cows characterized by granulomatous enteritis, chronic diarrhea, and eventually death. The disease is prevalent in the United States and worldwide, causing an estimated annual loss of more than $200 million for the dairy industry in the United States alone (21), and is considered one of the most serious infectious diseases in dairy cattle worldwide (8, 12). Both clinically ill and healthy but infected animals can shed *M. avium* subsp. *paratuberculosis* bacilli in their feces intermittently, exposing bacteria to variable adverse conditions such as low nutrients and variable temperatures. Contamination of the environment by the *M. avium* subsp. *paratuberculosis*-containing feces becomes the most common source of infection, especially for young calves who can be infected through the fecal-oral route (9). Clinically infected cows can shed 10^6 to 10^8 CFU/g of fecal material that can easily spread the infection to new calves, for which the infectious dose is 10^3 CFU/animal (51). Following the complete sequencing of the *M. avium* subsp. *paratuber-*

culosis genome (20), large-scale analysis of the genome contents of both clinical and environmental isolates of *M. avium* subsp. *paratuberculosis* identified several novel diagnostic targets (2, 29, 52). In this report, we test the hypothesis that profiling the gene expression patterns of *M. avium* subsp. *paratuberculosis* isolates exposed to different stress conditions or directly isolated from infected cows will provide insights into the genetic basis of virulence in *M. avium* subsp. *paratuberculosis*. Using a similar approach for stool samples of cholera patients, Larocque et al. (19) gained more insights into the pathogenesis of *Vibrio cholerae*.

Once reaching the intestinal lumen, virulent strains of *M. avium* subsp. *paratuberculosis* can invade intestinal tissue effectively within hours (53) and establish a persistent infection in the intestinal mucosa (26) and mesenteric lymph nodes, which can last for years (51). Earlier reports showed that *M. avium* subsp. *paratuberculosis* bacilli can survive and proliferate inside the phagosomes of infected macrophages by using mechanisms that are not completely understood (49). Preventing phagosome acidification is one of the possible scenarios by which *M. avium* subsp. *paratuberculosis* avoids macrophage killing (38). However, the genetic basis of such a mechanism of survival remains elusive. Recently, the expression profiles of the infected bovine macrophages were characterized to reveal different patterns of gene expression between cows clinically or subclinically infected with *M. avium* subsp. *paratuberculosis* (11). In this report, we profiled the mycobacterial response to several stress inducers (stressors) such as oxidative stress, heat shock, and acidic pH to mimic microenvironments that *M. avium* subsp. *paratuberculosis* bacilli might face during survival

---

* Corresponding author. Mailing address: Laboratory of Bacterial Genomics, Department of Pathobiological Sciences, University of Wisconsin—Madison, 1656 Linden Drive, Madison, WI 53706-1581. Phone: (608) 262-2861. Fax: (608) 262-7420. E-mail: atalaat@wisc.edu.
‡ Present address: Department of Microbiology, College of Medicine, Chungnam National University, Daejon 301-747, South Korea.

TABLE 1. PCR primers used in this study

Primer	Gene and direction	Purpose	Sequence
AMT137	accD5, forward	qRT-PCR	CTTCAACATCCCGATCATCA
AMT138	accD5, reverse	qRT-PCR	AGCCCATCACGCAGTAGG
AMT145	ptrBa, forward	qRT-PCR	CGGGTCTACGACATCGACTT
AMT146	ptrBa, reverse	qRT-PCR	CCGTAGCCGTAAATCAGTGC
AMT147	fabG3, forward	qRT-PCR	GTTACACCGCAACCAAATTC
AMT148	fabG3, reverse	qRT-PCR	TACACCACCAGGTTGGACAC
AMT817	tlyA, forward	qRT-PCR	CTGTCGTTCATCTCGCTGTG
AMT818	tlyA, reverse	qRT-PCR	CGCAGGAAGTATTCGACGTT
AMT819	lipM, forward	qRT-PCR	CTGGGTCAAACAACACATCG
AMT820	lipM, reverse	qRT-PCR	GATCGACTTGATCAGCAGTCC
AMT823	lipN, forward	qRT-PCR	TGGTTCGAATCGCAGTACCT
AMT824	lipN, reverse	qRT-PCR	CGAGCTGGAACAGGTTGG
AMT924	MAP4287c, forward	qRT-PCR	ATTGCACGCCTCCGATCT
AMT925	MAP4287c, reverse	qRT-PCR	CAGCACCGTCAGCGTCTC
AMT278	lipN upstream, forward	Gene knockout	ATATATACTAGTACCTTGGCGATGTACTTGC
AMT279	lipN upstream, reverse	Gene knockout	ATATATAAGCTTTCTGATCCATGCGACGGG
AMT280	lipN downstream, forward	Gene knockout	ATATATTCTAGAGGGTGCGGTGTCGGTCAG
AMT281	lipN downstream, reverse	Gene knockout	ATATATGGTACCGCCGGCCAGTGAATCAGG
AMT125	Hygromycin resistance gene, forward	Mutant confirmation	GGGAAGACCTCGGAATGG
AMT126	Hygromycin resistance gene, reverse	Mutant confirmation	CTGCGGAACGACCAGGAAT
AMT222	lipN_104, forward	Mutant confirmation	CGAACCCAGGTACCGCAG
AMT223	lipN_919, reverse	Mutant confirmation	ATGCTGTCCGGTCTGCGC

inside macrophages. We also took advantage of a relatively simple protocol to isolate a large number of *M. avium* subsp. *paratuberculosis* bacilli from clinically infected cows to define the transcriptional profile of *M. avium* subsp. *paratuberculosis* continuously shed in the feces. The latter analysis could uncover the transcriptional machinery of bacilli that are most likely to transmit infections to naïve animals. In general, our analysis identified the "stressome," the bacterial stress responses on a genome-wide level, employed by *M. avium* subsp. *paratuberculosis* to survive in hostile microenvironments. In addition, the contribution of a selected list of stress-responsive genes to *M. avium* subsp. *paratuberculosis* survival was examined in a mouse model of paratuberculosis, which identified a set of novel virulence factors including several lipases involved in lipid degradation in *M. avium* subsp. *paratuberculosis*.

MATERIALS AND METHODS

Bacteria. *M. avium* subsp. *paratuberculosis* ATCC 19698 was used for all in vitro transcriptional profiling. *M. avium* subsp. *paratuberculosis* K-10 was used only for generating the *lipN* mutant and for infecting a control group of mice. For all cultures, *M. avium* subsp. *paratuberculosis* ATCC 19698 and *M. avium* subsp. *paratuberculosis* K-10 were grown in Middlebrook 7H9 broth (Difco, Sparks, MD) supplemented with 0.5% glycerol, 2 μg/ml mycobactin J (Allied Monitor, Fayette, MO), 0.05% Tween 80, and 10% ADC (2% glucose, 5% bovine serum albumin fraction V, and 0.85% NaCl) at 37°C with shaking at 100 rpm/min. For animal inoculation, bacterial cultures of an optical density at 600 nm of 1.0 were harvested, washed once in phosphate-buffered saline (PBS), and resuspended in an equal volume of PBS. When needed, serial dilutions of *M. avium* subsp. *paratuberculosis* cultures were plated on 7H10 agar supplemented with 0.5% glycerol, 2 μg/ml mycobactin J, and 10% ADC. Agar plates for organ colony counting from animal tissues were also supplemented with 5 mg/ml vancomycin, 30 mg/ml amphotericin B, and 10 mg/ml nalidixic acid to reduce bacterial and fungal contamination, especially when intestines were plated.

RNA extraction from bacterial cultures. To profile the mycobacterial stress response to variable conditions, *M. avium* subsp. *paratuberculosis* ATCC 19698 cultures were allowed to grow to mid-log phase (optical density at 600 nm, 0.5) and aliquots were subjected to one of the following stressors: (i) shift to 45°C, (ii) addition of H_2O_2 to a final concentration of 10 mM, (iii) low pH obtained by adding HCl (pH 5.5), or (iv) treatment with hexadecylpyridinium chloride (HPC; Sigma, St. Louis, MO) to a final concentration of 1%. Measuring the pH of 1%

HPC solution indicated its acidity to be pH 5.0. All cultures were exposed to each treatment for 3 h before bacterial pellets were harvested by centrifugation at $3,200 \times g$ for 20 min. Total RNA from mycobacterial cultures was extracted using protocols that we established before with a few modifications (44, 45). Briefly, bacterial pellets (10^7 to 10^8 CFU) were resuspended in 4 ml TRIzol reagent (Invitrogen, Carlsbad, CA), split into four 2-ml screw-cap tubes each with 3.0 g of 0.1 mm zirconia/silica beads (BioSpect Products, Inc.), and disrupted in a Mini-BeadBeater-8 (BioSpect Products, Inc.) at top speed four times for 30 s each with 30-s intervals on ice. Following a 10-min incubation at room temperature, the supernatant was transferred to RNase-free tubes and centrifuged at 11,000 rpm for 15 min. RNA was isolated from the supernatant with chloroform and isopropanol treatments, washed with 75% ethanol, air dried, and resuspended in RNase-free H_2O as described before (45). To remove contaminating DNA, RNA samples were treated with DNase I (Invitrogen) (10 U/μg) at 37°C for 30 min. The quality and quantity of the extracted RNA were examined with agarose gel electrophoresis (see Fig. S1 in the supplemental material) and an Ultrospec 3100 *pro* UV/Visible spectrophotometer (GE Healthcare, Piscataway, NJ).

Cow fecal samples. Feces from Holstein cows with a documented history of Johne's disease were collected by the Johne's Testing Center, University of Wisconsin—Madison. Before mycobacterial culturing or direct isolation of RNA, 3 g of fecal samples was treated with 30 ml of 1% HPC for 16 h to eliminate fungal and nonmycobacterial contaminants. This procedure was used before to decontaminate *M. avium* subsp. *paratuberculosis*-contaminated samples (16, 31). The upper liquid layer was carefully transferred and centrifuged at $3,200 \times g$ for 20 min to harvest mycobacterial pellets from infected animals. These bacterial pellets (10^7 CFU) were directly used for RNA extraction without further enrichment or addition of antibiotic. At least 10 bacterial pellets were collected from each cow to obtain enough bacterial RNA for DNA microarray analysis. RNA was extracted from bacterial pellets as described above. To confirm the identity of the *M. avium* subsp. *paratuberculosis* bacilli isolated from the fecal samples, we used PCR to amplify IS*900* sequences from all bacterial pellets recovered from the feces (data not shown) before proceeding to RNA extraction. Additionally, DNase I-treated RNA isolated from cow samples was subjected to standard reverse transcription (46) and PCR amplification using specific primers for *tlyA*, *lipM*, and *lipN* genes (Table 1). These amplicons were further sequenced to confirm the identity of the amplified transcripts.

Microarray sample preparation and hybridization. For all microarray experiments, tiled-oligonucleotide DNA microarrays designed from the genome sequence of *M. avium* subsp. *paratuberculosis* K-10 were constructed by NimbleGen Systems Inc. (Madison, WI) (37, 52). Attempts were made to design 14 unique pairs of 24-mer oligonucleotides covering 100% of the predicted open reading frames (ORFs) in the *M. avium* subsp. *paratuberculosis* genome (20). However, because of the large number of sequence repeats in the *M. avium* subsp. *para-*

tuberculosis genome, only 91.2% of *M. avium* subsp. *paratuberculosis* predicted ORFs were used to construct the *M. avium* subsp. *paratuberculosis* DNA microarrays. For every perfect match probe of the ORF sequence, there is a corresponding mismatch probe with mutations at the 6th and 12th positions. For each hybridization, total RNA samples were reverse transcribed to cDNA and fluorescently labeled according to a protocol established earlier by our group and NimbleGen (37, 52). Briefly, RNA (5 μg) was incubated with 0.5 μg of random nonamer, 0.01 mM of dithiothreitol, 1 mM of deoxynucleoside triphosphates, and 300 U of SuperScript II reverse transcriptase (Invitrogen) at 42°C for 90 min. The remaining RNA was removed by adding NaOH, and the pH was equilibrated by adding HEPES. The generated cDNA was randomly fragmented with 0.1 U of DNase I at 37°C for 5 to 10 min and purified with Millipore YM-10 microfilters (Billerica, MA). The fragmented cDNA was labeled with biotin using terminal deoxynucleotide transferase (Promega, Madison, WI) in the presence of 1 μM of biotin-N_6-ddATP (Perkin-Elmer Life Sciences Inc., Boston, MA) at 37°C for 1 h. Hybridizations were conducted using NimbleGen hybridization chambers as described before (52) by adding biotin-labeled samples heated to 95°C for 5 min. After 12 to 16 h of hybridization, the slides were washed in nonstringent (6× SSPE [1× SSPE is 0.18 M NaCl, 10 mM NaH$_2$PO$_4$, and 1 mM EDTA (pH 7.7)] and 0.01% Tween 20) and stringent (100 mM morpholineethanesulfonic acid, 0.1 M NaCl, and 0.01% Tween 20) buffers for 5 min each followed by adding Cy3-streptavidin (GE Healthcare). An Axon GenePix 4000B laser scanner (Axon Instrument, Union City, CA) was used to scan the slides at 5-μm resolution.

Data analysis. Hybridization signals were extracted from the scanned images using the NimbleScan software (NimbleGen). The signal intensity of each ORF was represented by the mean of the 14 probe signals calculated by subtracting mismatch signals from perfect match signals to eliminate background signals. Two hybridizations from two biological replicates of each examined condition were analyzed with a total of 28 data points collected for each examined ORF. Raw hybridization signals were normalized by scaling the mean signal for each array to 1,000. Signal intensities of <5 were transformed to 5 to accommodate genes with undetectable transcripts in one treatment but not the others. The normalized linear signals were loaded to the R program (http://www.r-project.org/) with the EBarrays package, which employs empirical Bayes statistics to identify differentially expressed genes between two conditions by calculating the posterior probability of differential expression using the Lognormal-Normal model (17). Differential gene expression was considered significant only if genes have a probability of differential expression of >0.5 and a change of >±2-fold. Normalized signal intensities were also analyzed using hierarchical clustering algorithms implemented in TIGR Multi-Experiment Viewer software 4.0b (http://www.tigr.org/software/microarray.shtml).

Quantitative PCR. For a selected list of genes (Table 1), we performed a SYBR green-based, quantitative real-time PCR (qRT-PCR) to evaluate the performance of the DNA microarrays. To confirm the absence of genomic DNA in the RNA sample used for qRT-PCR, IS*900*-specific primers were used to amplify RNA samples. Only IS*900* amplicon-negative RNA samples were allowed for subsequent qRT-PCR analysis. The templates for qRT-PCR (cDNA) were prepared as described above for DNA microarray analysis. All primers used here (Table 1) were designed with web-based tools, Primer3 (http://frodo.wi.mit.edu/cgi-bin/primer3/primer3_www.cgi), and analyzed using the BLAST algorithm against the whole GenBank database to confirm their specific binding to the target sequences (E scores were <0.05 for primers that were >18-mers). PCRs were prepared using Bio-Rad (Hercules, CA) iQ-SYBR Green Supermix and run using the 7300 Real-Time PCR System (Applied Biosystems, Foster City, CA). The threshold cycle (C_T) of each gene was normalized to the C_T of the 16S rRNA from the same cDNA sample. The expression changes (*n*-fold) were calculated by comparing the normalized C_T of treated samples to that of the control sample as previously detailed (48).

Construction of *lipN*-knockout mutant. The specialized transduction protocol used earlier for *Mycobacterium tuberculosis* (4) was employed to generate an in-frame deletion of 1.1 kb of the *lipN* gene from *M. avium* subsp. *paratuberculosis* strain K-10. Briefly, the *lipN* allelic-exchange substrate was generated using the pYUB854 shuttle vector. Fragments of ~700 bp upstream and downstream of the *lipN* coding region were amplified with primers (Table 1) that introduced restriction sites compatible with the cloning sites in pYUB854. Restriction enzyme-digested amplicons representing both the left and right flanking regions of *lipN* were gel purified using the Wizard Gel Clean-Up System (Promega) and subsequently cloned into pYUB854 to generate the pYUB854::*lipN* construct. The DNA of the temperature-sensitive phasmid phAE87 (3) was self-ligated to generate concatemers and subsequently digested with PacI. DNA of the pYUB854::*lipN* construct was also digested with PacI and ligated with digested phAE87 concatemers to replace the pYUB328 cosmid sequence using an in vitro

lambda-packaging system (GIGAPackII; Stratagene, La Jolla, CA). The packaged phage particles were transduced into *Escherichia coli* HB101, and the shuttle phasmid DNA was extracted from the mixture of hygromycin-resistant colonies. *Mycobacterium smegmatis* cells were transformed with the purified phasmid DNA by electroporation, and the transformants were allowed to produce plaques at 30°C. The recombinant mycobacteriophage in the lysate was subsequently propagated and titrated in *M. smegmatis*. High-titer phage constructs were further transduced to *M. avium* subsp. *paratuberculosis* K-10 at the nonpermissive temperature (37°C) with a multiplicity of infection of 10. The genotype of *lipN*-deletion mutants growing on hygromycin-containing plates was confirmed with PCR and Southern blotting analyses as outlined before (36, 47).

Virulence assay of *M. avium* subsp. *paratuberculosis* mutants in mice. BALB/c mice were purchased from Harlan (Indianapolis, IN) at 3 weeks of age and kept in a pathogen-free environment according to our approved protocol from the Institutional Animal Care and Use Committee, University of Wisconsin—Madison. Groups of mice (*n* = 10 to 20 each) were inoculated with either *M. avium* subsp. *paratuberculosis* K-10 or one of its isogenic mutants generated by homologous recombination (Δ*lipN* strain) or insertional mutagenesis (Δ*lipL*, Δ*aceAB*, Δ*mbtH2*, Δ*prrA*, and Δ*lpqP* strains) selected from a previous analysis of an *M. avium* subsp. *paratuberculosis* mutant library (36). All insertional mutants were constructed in *M. avium* subsp. *paratuberculosis* ATCC 19698 as described before (36). PBS-washed and resuspended bacteria were dispersed using a cup-horned sonicator (Fisher Scientific, Pittsburgh, PA) and injected into the mice intraperitoneally. Inocula were adjusted to yield a dose of 10^7 to 10^8 CFU/mouse. Mouse groups (*n* = 3 to 6) were sacrificed at 3, 6, and 12 weeks postinfection (WPI), and samples from liver and intestine were collected for bacterial and histopathological examinations as previously described (36).

RESULTS

***M. avium* subsp. *paratuberculosis* responses to variable stress conditions.** Following oral infection, *M. avium* subsp. *paratuberculosis* bacilli face variable microenvironments during translocation across the alimentary tract to reach their final destination in the macrophages (53). To gain insights into bacterial responses upon exposure to stressors, we examined the transcriptional profile of *M. avium* subsp. *paratuberculosis* cultures following treatments with defined stimuli such as acidic pH, heat shock, or oxidative stress using tiled-oligonucleotide DNA microarrays. Heat treatment at 45°C was chosen to identify the general stress response of *M. avium* subsp. *paratuberculosis*, while acidic pH and oxidative conditions were chosen to profile *M. avium* subsp. *paratuberculosis* exposure to the environment of the abomasums or within macrophages, respectively. The 3-h exposure time was selected based on the rapid change in gene transcripts in bacteria (30, 54) and the complex nature of the mycobacterial cell wall that controls the flow of stressors. A similar time frame was employed before for *M. tuberculosis* cultures (34, 50). Preliminary analysis of the hybridization replicates revealed a high level of correlation among biological replicates (*r* > 0.8) (Fig. 1A) with detectable levels of hybridization in >70% of all the ORFs carried in the *M. avium* subsp. *paratuberculosis* K-10 genome (see Table S1 in the supplemental material). Considering all of the ORFs with detectable hybridization signals (above background level) in at least one of the examined samples indicated the presence of transcripts in all ORFs examined by DNA microarrays (91.2% of the included ORFs). It is noteworthy that not all detected transcripts were significantly regulated (see below). The detection of such a high percentage of transcripts confirms the gene predictions used for the *M. avium* subsp. *paratuberculosis* genome (20). qRT-PCR analysis of a selected list of genes further confirmed the regulation of 85% of the examined genes, consistent with their regulation estimated by DNA microarrays (see Table S2 in the supplemental material).
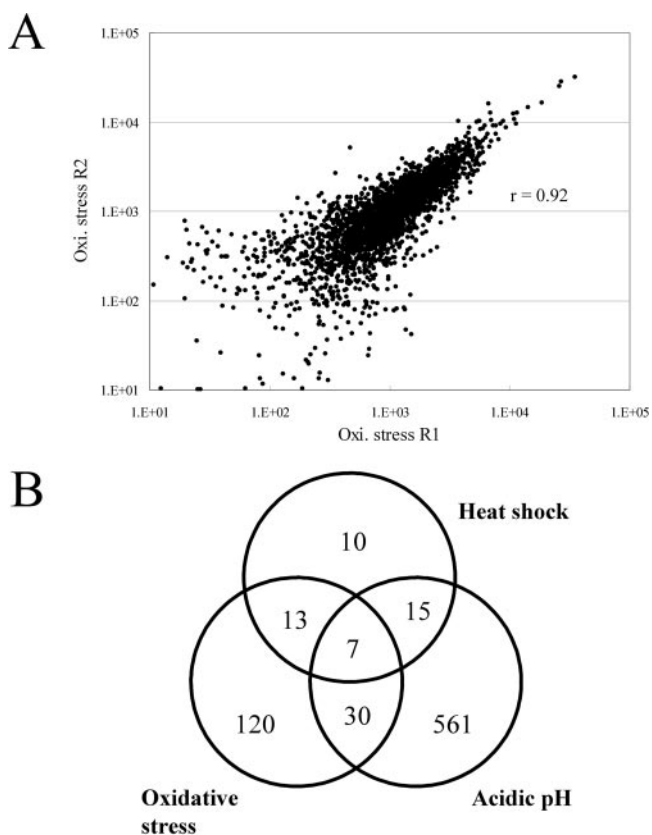
A

B

FIG. 1. Microarray analysis of *M. avium* subsp. *paratuberculosis* cultures exposed to variable stressors. (A) A scatter plot analysis displaying a high reproducibility between biological replicates ($r > 0.9$) of *M. avium* subsp. *paratuberculosis* cultures following exposure to oxidative stressors. (B) Venn diagram of genes that significantly changed expression levels under various in vitro stress conditions.

Of the three profiles examined with DNA microarrays, the low-pH-treated samples had the largest number of genes with significantly altered expression levels ($n = 597$) compared to untreated samples. Heat shock and oxidative stress gave lower numbers of significantly regulated genes (31 and 155, respectively) (see Tables S3, S4, and S5 in the supplemental material). As expected, the shift in culture temperature to 45°C induced a set of genes such as *dnaK*, *dnaJ*, *htpX*, *groEL1*, *groEL2*, and *hsp18*. Heat shock of *M. tuberculosis* induced responses in orthologous genes similar to those in the previously mentioned list (42, 43), further validating the DNA microarrays used for gene expression profiling. Genes encoding several regulatory factors (based on sequence annotation) were also up-regulated (e.g., MAP3575, MAP0661c, and MAP3331), suggesting the activation of an array of heat shock-responsive genes. Similarly, transcriptional levels of several other regulatory genes were altered significantly during exposure to oxidative and low-pH treatments. Specifically, one of the extracytoplasmic sigma factors, *sigH*, was up-regulated by the oxidative stress, consistent with an earlier finding in *M. tuberculosis* (32). In addition, *35kd_ag* (MAP2855c) and a gene encoding a regulatory protein, *whiB2*, were among the significantly induced genes under oxidative stress. Previously, *whiB2* and *35kd_ag* were up-regulated during nutrient starvation (5)

and heat shock (43) in *M. tuberculosis*, respectively, suggesting that these two genes could play a role in relief of the oxidative stress in *M. avium* subsp. *paratuberculosis*. Conversely, another sigma factor, *sigD*, was down-regulated when acidic-pH samples were examined. In fact, the majority of the significantly regulated genes were down-regulated ($n = 402$), while only 195 genes were up-regulated at acidic pH. This profile was similar to the one generated by *M. tuberculosis* following exposure to low pH (14). Among the up-regulated genes are those involved in mycobactin metabolism (*mbtC*) and general stress-responsive genes such as *htpX*, *clpX*, and *relA*. The high number of regulated genes following exposure to low pH, in addition to the type of activated gene (i.e., stress-responsive genes), emphasized the importance of change in pH to the pathogenesis of *M. avium* subsp. *paratuberculosis*.

Further analysis of genes with a significant change in transcription levels under all examined stressors (Fig. 1B) identified a list of seven genes that were shared among all treatments. Only one gene in this list, MAP3430 (*pmmB*), was down-regulated, while the other six genes were up-regulated including the heat shock-responsive genes (*htpX*, *dnaJ*, and *groEL2*) (43) and the essential genes *infB* and *pmmA* in *M. tuberculosis* (33). Genes with unknown functions (MAP2720c and MAP0156) were also included in this list. Earlier microarray analysis (43) of *M. tuberculosis* cultures exposed to high temperature implicated four of these genes (*htpX*, *dnaJ*, *groEL2*, and *infB*) in the heat shock response. This profile suggests a common pathway involving these genes in response to stressors in both *M. avium* subsp. *paratuberculosis* and *M. tuberculosis*.

Transcriptional profiling of *M. avium* subsp. *paratuberculosis* isolated from naturally infected cows. Because fecal-oral transmission is the expected route of *M. avium* subsp. *paratuberculosis* infection in cattle, it is of great importance to understand the gene expression pattern of *M. avium* subsp. *paratuberculosis* bacilli shed in feces. We hypothesized that genes responsible for the persistence of *M. avium* subsp. *paratuberculosis* in feces could contribute to *M. avium* subsp. *paratuberculosis* virulence during infection. The whole-genome microarray approach was used to analyze in vitro cultures and bacterial pellets collected from fecal materials of infected cows. Both clinical signs and continuous shedding of *M. avium* subsp. *paratuberculosis* by the sampled cows confirmed their late stage of Johne's disease. During the recovery of *M. avium* subsp. *paratuberculosis* from the fecal samples, HPC treatment was used to eliminate nonmycobacterial contaminants (16, 31). Culturing of the decontaminated fecal samples indicated an *M. avium* subsp. *paratuberculosis* load of 10^7 CFU/gram of fecal sample, suggesting a good possibility for directly isolating *M. avium* subsp. *paratuberculosis* and purifying bacterial RNA for DNA microarrays. Nonetheless, a few bacterial colonies were isolated from fecal pellets when LB medium was used to culture fecal samples. To confirm the identity of transcripts isolated from fecal cow samples, amplicons were sequenced from purified RNA samples (see Fig. S1 in the supplemental material) following reverse transcription. In all examined genes ($n = 3$), BLAST analysis indicated their identity to be *M. avium* subsp. *paratuberculosis* or *M. avium* subsp. *avium* and not any other bacterial genes (Table 2). Because we examined only a small number of genes, we cannot confirm that all

TABLE 2. List of gene transcripts examined by reverse
transcriptase PCR and sequence analysis

Gene name	Amplicon size (bp)	E value		
		M. avium subsp. *paratuberculosis*	*M. avium*	Other bacteria
MAP1401, *tlyA*	263	2.0E-83	4.0E-80	No hit
MAP2041, *lipM*	247	3.0E-55	3.0E-50	No hit
MAP3006c, *lipN*	238	4.0E-59	9.0E-56	No hit

transcripts identified in the fecal samples were generated from *M. avium* subsp. *paratuberculosis*. Previously, decontamination with HPC was shown to greatly reduce bacterial and fungal contaminants but with little or no effect on the recovery of viable *M. avium* subsp. *paratuberculosis* (16, 31). As a control, the transcriptional profile of HPC-treated cultures was also analyzed to delineate the impact of using HPC on *M. avium* subsp. *paratuberculosis* transcripts during our protocol for sample decontamination.

To our surprise, microarray analysis of HPC-treated samples identified significant change in a large number of gene transcripts ($n = 649$), where most of the general stress-responsive genes observed in acidic pH or heat shock were also induced (e.g., *mbtC*, *relA*, *htpX*, and *hsp18*) (see Table S6 in the supplemental material). Accordingly, all of the data generated from the cow samples were compared to HPC-treated cultures to neutralize the effect of HPC treatment on *M. avium* subsp. *paratuberculosis*. Interestingly, transcriptional analysis of cow samples identified the largest number of genes ($n = 1,082$) that were significantly different from the HPC-treated samples (see Table S7 in the supplemental material). Among the highly activated genes are those involved in the survival of *M. tuberculosis* during chronic infection (e.g., *ung* and *icl* encoding isocitrate lyase) (25, 48) or those involved in nitrate reduction (*narH*) (40). Other genes included those involved in lipid metabolism such as *lipN* and *lipI*, suggesting a unique nutrient requirement for *M. avium* subsp. *paratuberculosis* isolated from fecal samples. Genes involved in variable DNA repair mechanisms (e.g., *lexA* and *uvrD2*) or heat shock (*htpG*) were among the group of up-regulated genes. However, other general stress-responsive genes were among the group of repressed genes such as *relA*, *hsp18*, and *clpB* and the transcriptional regulator *whiB3*, indicating the unique nature of the *M. avium* subsp. *paratuberculosis* strains isolated from cow samples. Finally, two sigma factors (*sigI* and *sigG*) were among the significantly induced genes in cow samples. In *M. tuberculosis*, only *sigI* was induced following exposure to mild cold (22), suggesting an adaptive response of *M. avium* subsp. *paratuberculosis* in feces to a lower temperature than that of the host (normal body temperature for a cow is 39°C). Overall, both the large number of genes regulated in *M. avium* subsp. *paratuberculosis* isolated from the cow samples and the type of activated/repressed genes portrayed bacilli that shared common features with in vitro-treated cultures but maintained a group of unique genes that were regulated only in the cow samples.

Grouping the stress-responsive genes. Analysis of significantly regulated genes of *M. avium* subsp. *paratuberculosis* in samples collected from cows or exposed to defined stressors identified a significantly large number of genes involved in

mycobacterial stress response to variable stimuli (almost 25% of the encoded genes). Further analysis of genes based on their transcriptional patterns could identify gene groups coregulated to perform a similar function. In this analysis, all genes with detectable levels of transcription (genes with hybridization signals higher than background level) were included and displayed a high level of correlation among all conditions examined (Fig. 2A). Consequently, we applied a hierarchical clustering algorithm (13) to identify unique transcriptional patterns of *M. avium* subsp. *paratuberculosis* genes during exposure to individual stressors. Based on the overall clustering of the transcripts, the profile of the cow samples was different from all in vitro cultures examined. The profile of the acidic-pH samples was closely related to that of the HPC-treated samples, and both profiles occupied a cluster node related to that of the cow fecal samples (Fig. 2B). On the other hand, samples exposed to either oxidative stress or heat shock were in a separate cluster node, suggesting a different profile for these conditions compared to the cow samples. Interestingly, one of the recently identified virulence factors in *M. avium* subsp. *paratuberculosis* (36), the *kdpC* gene, was clustered among a group of genes activated only in the cow samples. Other genes in this cluster included a fatty acid degradation lipase/esterase (*lipN*) and an orthologue to an *M. tuberculosis* virulence gene, *mmpl2* (7). It is possible that this cluster of genes is also involved in *M. avium* subsp. *paratuberculosis* virulence.

At the gene level, the employed clustering algorithm identified groups of coregulated genes that were shared among stress conditions, such as low pH and HPC treatment (see Table S8 in the supplemental material). In both samples, genes involved in mycobactin biosynthesis (*mbtH2*), mycolic acid biosynthesis (*cmaA2*), and a protein kinase (*pknB*) were induced, suggesting a potential role for their encoded proteins in the acidic response. Other genes that were shared among acidity, HPC treatment, and the cow samples included *mce1_1* and *mce4* (both involved in cell entry), *atpC*, and a transcriptional regulator gene, *kdpE*, suggesting a role of this group of genes in response to acidic pH during infection. Following exposure to low pH, 63% of the orthologous genes that were regulated by acidity in *M. avium* subsp. *paratuberculosis* and *M. tuberculosis* ($n = 36$) were also repressed (14) in both organisms, suggesting similar responses to acidity. Examples of the repressed genes include *fadE12*, *murA*, and *aspB*. Additionally, we compared the oxidative response of *M. tuberculosis* (34) to the one obtained in *M. avium* subsp. *paratuberculosis*. Among the gene groups that were regulated by H_2O_2 in *M. tuberculosis* (32), 25 to 38% of *M. avium* subsp. *paratuberculosis* gene orthologues were also induced or repressed, respectively, by the addition of H_2O_2. Examples of the shared activated genes include *sigH*, *sigB*, *icl*, *trxB2*, and *katG* (see Table S8 in the supplemental material). Taken together, the shared profiles indicated conserved responses to acidity and oxidative radicals usually present in mycobacterial environments, such as within macrophages (39).

To gain insights into the regulation of genetic networks in the stressome, gene clusters were inspected for genes coregulated with sigma factors, the global transcriptional regulators. A total of 19 sigma factors are predicted in the genome of *M. avium* subsp. *paratuberculosis*, where only *sigA* and *sigB* are considered essential sigma factors, while the rest are consid-
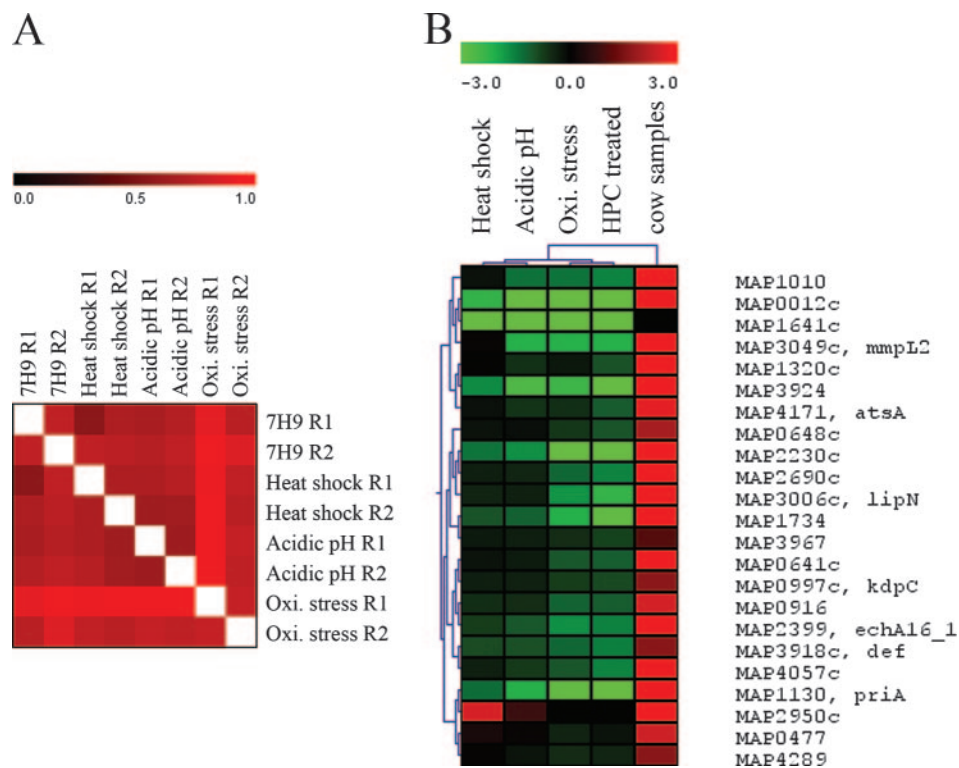
FIG. 2. Hierarchical cluster analysis of the gene expression levels collected from *M. avium* subsp. *paratuberculosis* cultures exposed to variable stressors. (A) A heat map displaying the overall correlation among replicates of all examined stressors. (B) An example of cluster analysis showing genes activated only in the cow samples. Note the dendrogram displayed at the top of the image reflecting the overall relationship among examined samples. A color bar is presented at the top of each panel with a range from 0 to 1 (black to red) for panel A or from −3 to 3 (green to red) for panel B.

ered extracytoplasmic (20). Seven extracytoplasmic sigma factors, *sigD*, *sigF1*, *sigG*, *sigH*, *sigI*, *sigL*, and ECF-6, were significantly regulated >±2-fold under any particular stressor, confirming their participation in regulating several gene groups. For example, cluster analysis identified a group of 71 *M. avium* subsp. *paratuberculosis* genes that were coexpressed with *sigD* while another group of 77 genes were coexpressed with *sigG*. Both gene groups were activated only in cow samples compared to the rest of the examined samples. Interestingly, both sigma factors were shown to be involved in *M. tuberculosis* virulence during chronic infection (*sigD*) (6) or survival in the macrophage (*sigG*) (15). Overall, cluster analysis portrayed both unique and common features of *M. avium* subsp. *paratuberculosis* responding to variable stimuli. The identified profiles also suggested the involvement of several highly regulated gene groups that could contribute to *M. avium* subsp. *paratuberculosis* virulence and pathogenesis under control of a set of sigma factors such as *sigD*, *sigE*, and *sigH*.

Stress-responsive genes are important for *M. avium* subsp. *paratuberculosis* survival in animals. As suggested by differential gene expression and hierarchical clustering, several genes displayed unique patterns of expression depending on the examined stressor. To test the hypothesis that stress-regulated genes contribute to *M. avium* subsp. *paratuberculosis* survival, we employed a strategy based on selecting mutants with inactivation/deletion of genes induced under stress conditions. These genes were tested for survival in a murine model of

paratuberculosis. The *lipN* gene, which was up-regulated in the cow samples, was targeted for deletion mutagenesis (4) as a representative of genes involved in lipid degradation. In *M. tuberculosis*, a mutant of the *lipF* gene that is a homolog to *M. avium* subsp. *paratuberculosis lipN* had an important effect on mycobacterial persistence in mice (18). Using homologous recombination, a 1.1-kb DNA fragment of the *lipN* coding region was replaced with a hygromycin-resistant gene cassette using *M. avium* subsp. *paratuberculosis* K-10 (4). The deletion of *lipN* was verified by both PCR and Southern blot analysis (Fig. 3), confirming the ability of the specialized transduction system developed for *M. tuberculosis* to knock out genes in *M. avium* subsp. *paratuberculosis*. To test the virulence of the generated mutant, we compared the colonization levels and histopathology of mice infected with the Δ*lipN* mutant to the wild-type strain of *M. avium* subsp. *paratuberculosis* K-10. Additionally, we used the same murine model to assess the virulence of a selected list of *M. avium* subsp. *paratuberculosis* mutants generated in *M. avium* subsp. *paratuberculosis* ATCC 19698 and identified during a large-scale screening of *M. avium* subsp. *paratuberculosis* transposon mutants (36). All of the examined mutants have insertions in genes that were up-regulated in vivo (*lipL* and *lpqP*) or in acidic pH (*prrA*, *aceAB*, and *mbtH2*) to variable degrees (Table 3). Figure 3D displays the location of disrupted genes in the examined mutants.

Interestingly, the colonization levels of all examined mutants (*n* = 6) were highly reduced compared to the wild-type strains
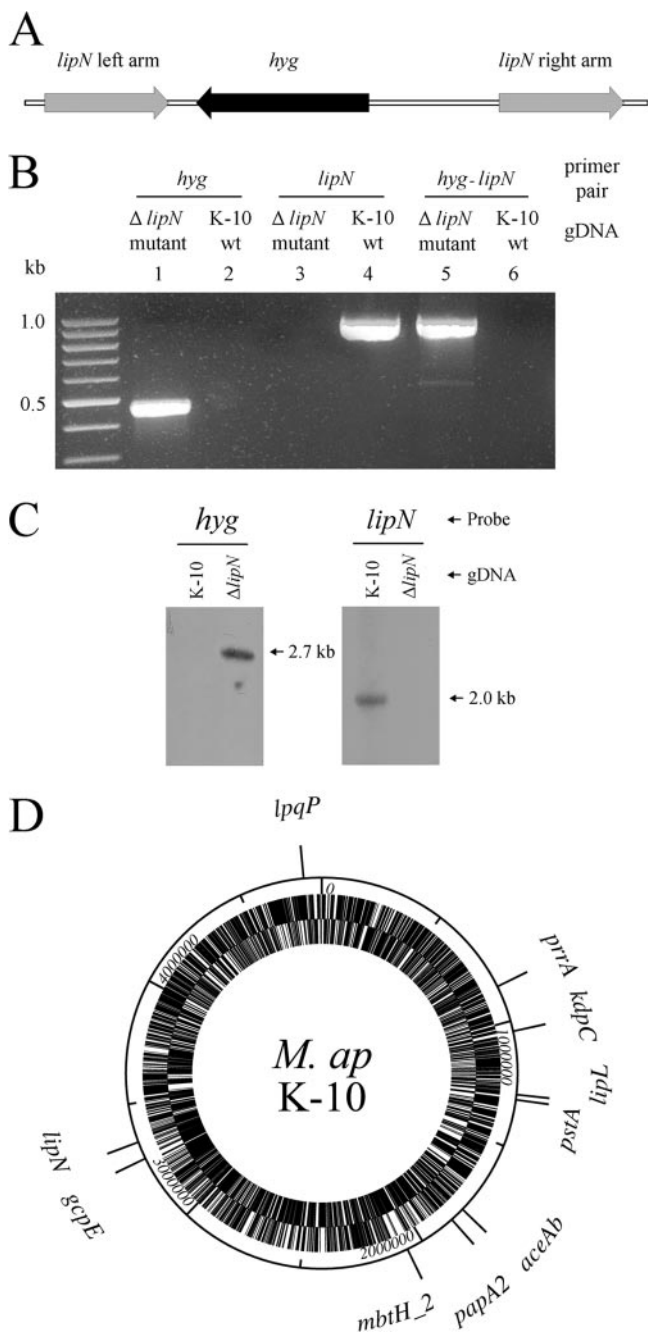
FIG. 3. Gene deletion in *M. avium* subsp. *paratuberculosis*. (A) The design of *lipN*-knockout allelic-exchange substrates using the pYUB854 cloning vector (4). (B) PCR confirmation of the *lipN*-knockout mutant using genomic DNA (gDNA) from the wild type (wt) and the Δ*lipN* mutant and primer pairs designed for the hygromycin resistance gene, *lipN*, or the recombinant region after allelic exchange. A 2% agarose gel showed amplicons from the hygromycin resistance gene only when the mutant genomic DNA was used (lane 1), whereas the *lipN* sequence was amplified only from the wild-type genomic DNA (lane 4). (C) Southern blot analysis of the *lipN*-knockout mutant. Genomic DNA was digested with XhoI and Acc65I (for hygromycin detection) or XhoI and ScaI (for *lipN* detection) and detected with hygromycin or *lipN* probes. The *lipN* sequence was absent from the *lipN*-knockout mutant genomic DNA. (D) A genomic map showing the distribution of the 10 genes inactivated by transposon mutagenesis or homologous recombination examined in this and previous studies (36, 53).

TABLE 3. Changes in expression of the list of genes selected for further screening of their mutants in mice[a]

Gene name	Low-pH group		Cow samples	
	Fold change	PDE	Fold change	PDE
MAP0834c, *prrA*	**3.55**	0.07	−35.71	0.64
MAP1228, *lipL*	−1.91	0.11	**34.34**	0.52
MAP3006c, *lipN*	−3.36	0.10	**33.79**	0.55
MAP1643, *aceAB*	**282.3**	0.85	−32.87	0.31
MAP1872c, *mbtH2*	**5.26**	0.10	−3.97	0.09
MAP4288, *lpqP*	−4.28	0.11	**4.94**	0.13

[a] Change (*n*-fold) with posterior differential of expression (PDE) is listed based on Bayesian statistical analysis. Bold indicates positive values for change (*n*-fold).

(Fig. 4), at least at one time point of the infection. The Δ*lipN* mutant was consistently cleared from livers and intestines of mice, especially by 12 WPI compared to its parent strain, *M. avium* subsp. *paratuberculosis* K-10. Other mutants regained some of the colonization levels after 6 WPI (e.g., *mbtH2* and *lipL*), suggesting the contribution of the disrupted genes to the initial stages of infection. It is also noteworthy that colonization levels of both *M. avium* subsp. *paratuberculosis* ATCC 19698 and K-10 were similar at 3 and 6 WPI but not at 12 WPI. Histopathological analysis of liver sections of infected animals showed a lower level of granuloma formation compared to the result from mice infected with the wild-type strain (see Fig. S2 in the supplemental material), verifying the attenuated phenotype indicated by the colonization data. In addition, more granulomas were observed in mutants with higher bacterial counts in the organs. Overall, screening of the *M. avium* subsp. *paratuberculosis* mutants in the murine model of paratuberculosis suggested the participation of *lipL* and *mbtH2* in the initial stage of infection. However, the rest of the genes (*lipN*, *lpqP*, *aceAB*, and *prrA*) could participate in tissue colonization throughout early and late infection. Previously, *M. avium* subsp. *paratuberculosis* mutants with insertional mutations in *pstA*, *kdpC*, *gcpE*, and *papA2* genes (Fig. 3D) were attenuated in the murine model of paratuberculosis (36). Interestingly, the former three genes were induced by 67.1-, 3.2-, and 88.2-fold in the cow samples compared to the in vitro samples, respectively, while *papA2* was induced by 4.6-fold at low pH. When tested in a calf model of intestinal invasion, the Δ*pstA* mutant was also attenuated (53). Overall, mutants with disruption/deletion of genes highly induced in cow feces or acidic-pH samples were attenuated in the murine model of paratuberculosis, suggesting a key role for these two classes of genes in *M. avium* subsp. *paratuberculosis* survival during infection.

DISCUSSION

For a long time, the molecular basis of the pathogenesis of *M. avium* subsp. *paratuberculosis* infection has not been completely understood, despite the great economic impact of Johne's disease on the dairy industry (21) and the potential involvement of *M. avium* subsp. *paratuberculosis* in Crohn's disease in humans (27). Fortunately, with the advance of genomic analysis of microbial pathogens, the genome sequence of *M. avium* subsp. *paratuberculosis* K-10 became available (20). This has sparked investigation of the genomic variations
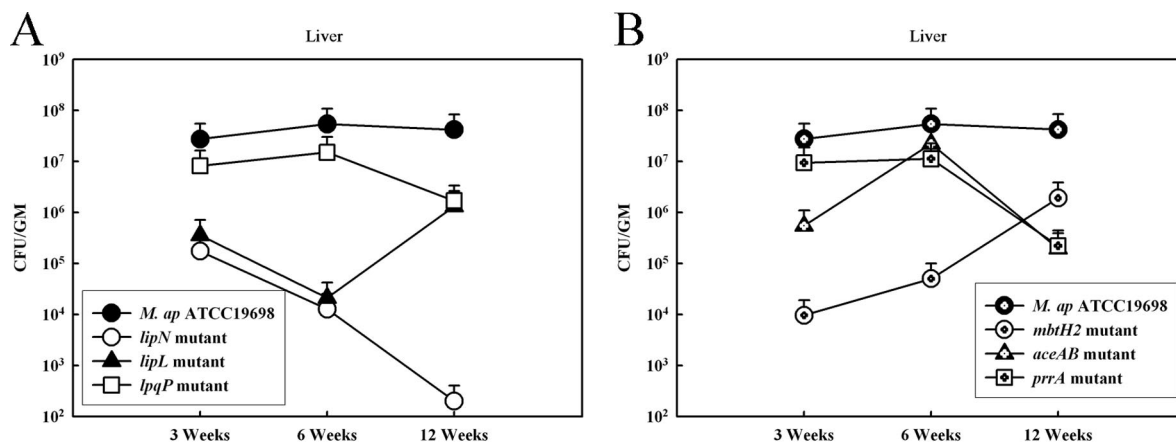
FIG. 4. Screening of *M. avium* subsp. *paratuberculosis* mutants in the murine model of paratuberculosis. Mouse groups were intraperitoneally inoculated with 10^8 CFU/mouse for the *M. avium* subsp. *paratuberculosis* ATCC 19698 wild-type strain or its isogenic mutant while groups inoculated with *M. avium* subsp. *paratuberculosis* K-10 or its $\Delta lipN$ isogenic mutant were inoculated with 10^7 CFU/mouse. Liver and intestine tissues were collected at 3, 6, and 12 WPI. Only data for the liver are shown here. (A) Colonization levels of three mutants with disruption of genes activated in cow samples compared to levels obtained from mouse groups infected with either *M. avium* subsp. *paratuberculosis* ATCC 19698 or *M. avium* subsp. *paratuberculosis* K-10. (B) Colonization levels of three mutants with disruption of genes activated in acidic pH compared to levels obtained from a mouse group infected with the wild-type *M. avium* subsp. *paratuberculosis* ATCC 19698. Error bars represent standard errors ($\pm$) of colony counts from different samples at each time ($n = 3$ to 6).

among isolates of *M. avium* subsp. *paratuberculosis* and created novel diagnostic targets (2, 35, 52). Nonetheless, the regulation of expressed genes responsible for establishing infection on a genome-wide scale remained poorly understood. Here, we report the first effort to profile gene transcripts of *M. avium* subsp. *paratuberculosis* exposed to several stressors or isolated directly from infected cows. Although unique profiles emerged for *M. avium* subsp. *paratuberculosis* following exposure to stressors, there was a set of common genes that shared transcriptional levels among all examined stressors. This strongly indicates their involvement in the universal mycobacterial response to stress conditions including the family of heat shock proteins (e.g., *hsp* and *htpX*).

Surprisingly, a large number of genes were induced during exposure to acidic pH compared to other in vitro conditions, suggesting the importance of the change in pH to the survival of *M. avium* subsp. *paratuberculosis*. However, the largest number of regulated genes was identified when the transcriptional profile of *M. avium* subsp. *paratuberculosis* isolated from cow samples was analyzed, indicating the unique challenge for *M. avium* subsp. *paratuberculosis* in order to survive in the cow excreta. Such analysis is complicated by the potential presence of other bacterial transcripts despite the decontamination protocol that we used here. Also, variations among transcription profiles of clinical isolates and the standard strain (ATCC 19698) used for all in vitro stressors could further complicate the analysis of the cow samples. Finally, we realize that analyzing *M. avium* subsp. *paratuberculosis* isolated from fecal samples would not necessarily mimic the host microenvironments (i.e., cow intestine). However, feces- or host-adapted mycobacteria are the most efficient forms for transmitting infections to naïve animals as shown by both historical (1) and experimental (41) evidence. In fact, inactivation of the three genes that were induced in the fecal samples was detrimental to the survival of *M. avium* subsp. *paratuberculosis* in mice, which was similar to the results obtained from the inactivation

of genes up-regulated by low pH. Some mutants (e.g., $\Delta lipL$ and $\Delta mbtH2$ mutants) partially regained their ability to colonize livers by 12 WPI, suggesting the importance of these genes to initiating a successful infection. On the other hand, other mutants (e.g., $\Delta lipN$ and $\Delta prrA$ mutants) were not efficient in colonizing livers throughout the examined times, suggesting a potential role for these genes in establishing chronic infection. Further analysis is needed to verify the attenuation associated with the examined genes (e.g., complementation analysis) and to characterize the mechanisms of attenuation exhibited by each mutant in a better model for Johne's disease such as the calf model.

Throughout this report, we analyzed the transcriptional profiles of *M. avium* subsp. *paratuberculosis* in comparison to those previously reported for *M. tuberculosis* (14, 24, 43, 48). At this point, few experimental data are available for the transcriptional responses of *M. avium* subsp. *paratuberculosis*, which stifled our comparative analysis. Nonetheless, several common responses were found between *M. avium* subsp. *paratuberculosis* and *M. tuberculosis* at the transcriptional level (e.g., heat shock and oxidative responses), reflecting the conserved evolutionary relationship between the two types of mycobacteria. Also, it indicates the similarity between the two types of infections at the cellular level (e.g., both organisms survive the macrophage microenvironment). However, variations among transcriptional profiles were also found. In *M. tuberculosis*, only a small number of genes ($n = 81$) (14) compared to a large number of *M. avium* subsp. *paratuberculosis* genes ($n = 597$) were regulated under acidic pH. In contrast, a higher number of genes significantly responded to oxidative stress in *M. tuberculosis* ($n = 761$) (34) compared to only 155 genes in *M. avium* subsp. *paratuberculosis*. Such a difference between the two pathogens could reflect the disparity between the microarray platforms or protocols used by each laboratory. Such disparity in responses could also reflect a genuine difference between the microenvironments of the alveolar and enteric macro-

phages for *M. tuberculosis* and *M. avium* subsp. *paratuberculosis*, respectively.

In addition to common and unique *M. avium* subsp. *paratuberculosis* genetic circuits identified for each examined stressor, the employed transcriptional analysis confirmed the gene predictions of a large number of ORFs (91.2% of the genome). As previously suggested (23), environmental stressors usually induce different sigma factors depending on the nature of stimuli. Our microarray analysis suggested the involvement of *sigH* in the *M. avium* subsp. *paratuberculosis* response to oxidative and heat shock stressors as shown previously for *M. tuberculosis* (32). It is also possible that *sigD* and *sigG* participate in the persistent infection with *M. avium* subsp. *paratuberculosis* while *sigI* is involved in adaptation to cold shock, as suggested for *M. tuberculosis* (22). The rest of the sigma factors may not play a critical role under the examined stress conditions. More analysis is needed to further analyze the role of stress-induced genes in *M. avium* subsp. *paratuberculosis* survival during natural infection and to better understand the mechanisms used by *M. avium* subsp. *paratuberculosis* to survive in hostile microenvironments. Such knowledge will improve the ability to control *M. avium* subsp. *paratuberculosis* infections. Our strategy for transcriptional profiling and subsequent assessment of specific mutants in animal models of infection could be applied to other intracellular pathogens to elucidate their mechanisms of virulence.

REFERENCES

1. **Ayele, W. Y., M. Machäèková, and I. Pavlík.** 2001. The transmission and impact of paratuberculosis infection in domestic and wild ruminants. Vet. Med. **6–7:**205–224.
2. **Bannantine, J. P., E. Baechler, Q. Zhang, L. L. Li, and V. Kapur.** 2002. Genome-scale comparison of *Mycobacterium avium* subsp. *paratuberculosis* with *Mycobacterium avium* subsp. *avium* reveals potential diagnostic sequences. J. Clin. Microbiol. **40:**1303–1310.
3. **Bardarov, S., J. Kriakov, C. Carriere, S. W. Yu, C. Vaamonde, R. A. McAdam, B. R. Bloom, G. F. Hatfull, and W. R. Jacobs, Jr.** 1997. Conditionally replicating mycobacteriophages: a system for transposon delivery to *Mycobacterium tuberculosis*. Proc. Natl. Acad. Sci. USA **94:**10961–10966.
4. **Bardarov, S., M. S. Pavelka, V. Sambandamurthy, M. Larsen, J. Tufariello, J. Chan, G. Hatfull, and W. R. Jacobs.** 2002. Specialized transduction: an efficient method for generating marked and unmarked targeted gene disruptions in *Mycobacterium tuberculosis*, *M. bovis* BCG and *M. smegmatis*. Microbiology **148:**3007–3017.
5. **Betts, J. C., P. T. Lukey, L. C. Robb, R. A. McAdam, and K. Duncan.** 2002. Evaluation of a nutrient starvation model of *Mycobacterium tuberculosis* persistence by gene and protein expression profiling. Mol. Microbiol. **43:**717–731.
6. **Calamita, H., C. Ko, S. Tyagi, T. Yoshimatsu, N. E. Morrison, and W. R. Bishai.** 2005. The *Mycobacterium tuberculosis* SigD sigma factor controls the expression of ribosome-associated gene products in stationary phase and is required for full virulence. Cell. Microbiol. **7:**233–244.
7. **Camacho, L. R., D. Ensergueix, E. Perez, B. Gicquel, and C. Guilhot.** 1999. Identification of a virulence gene cluster of *Mycobacterium tuberculosis* by signature-tagged transposon mutagenesis. Mol. Microbiol. **34:**257–267.
8. **Cetinkaya, B., K. Egan, D. A. Harbour, and K. L. Morgan.** 1996. An abattoir-based study of the prevalence of subclinical Johne's disease in adult cattle in south west England. Epidemiol. Infect. **116:**373–379.
9. **Collins, D. M., A. J. Radford, G. W. De Lisle, and H. Billman-Jacobe.** 1994. Diagnosis and epidemiology of bovine tuberculosis using molecular biological approaches. Vet. Microbiol. **94:**83–89.
10. **Collins, M. T., D. C. Sockett, W. J. Goodger, T. A. Conrad, C. B. Thomas, and D. J. Carr.** 1994. Herd prevalence and geographic distribution of, and risk factors for, bovine paratuberculosis in Wisconsin. J. Am. Vet. Med. Assoc. **204:**636–641.
11. **Coussens, P. M., C. J. Colvin, K. Wiersma, A. Abouzied, and S. Sipkovsky.** 2002. Gene expression profiling of peripheral blood mononuclear cells from cattle infected with *Mycobacterium paratuberculosis*. Infect. Immun. **70:**5494–5502.
12. **De Lisle, G. W., G. F. Yates, and R. H. Montgomery.** 2003. The emergence of *Mycobacterium paratuberculosis* in farmed deer in New Zealand—a review of 619 cases. N. Z. Vet. J. **51:**58–62.
13. **Eisen, M. B., P. T. Spellman, P. O. Brown, and D. Botstein.** 1998. Cluster analysis and display of genome-wide expression patterns. Proc. Natl. Acad. Sci. USA **95:**14863–14868.
14. **Fisher, M. A., B. B. Plikaytis, and T. M. Shinnick.** 2002. Microarray analysis of the *Mycobacterium tuberculosis* transcriptional response to the acidic conditions found in phagosomes. J. Bacteriol. **184:**4025–4032.
15. **Graham, J. E., and J. E. Clark-Curtiss.** 1999. Identification of *Mycobacterium tuberculosis* RNAs synthesized in response to phagocytosis by human macrophages by selective capture of transcribed sequences (SCOTS). Proc. Natl. Acad. Sci. USA **96:**11554–11559.
16. **Grant, I. R., E. I. Hitchings, A. McCartney, F. Ferguson, and M. T. Rowe.** 2002. Effect of commercial-scale high-temperature, short-time pasteurization on the viability of *Mycobacterium paratuberculosis* in naturally infected cows' milk. Appl. Environ. Microbiol. **68:**602–607.
17. **Kendziorski, C. M., M. A. Newtone, H. Lan, and M. N. Goululd.** 2003. On parametric empirical Bayes methods for comparing multiple groups using replicated gene expression profiles. Stat. Med. **22:**3899–3914.
18. **Lamichhane, G., M. Zignol, N. J. Blades, D. E. Geiman, A. Dougherty, J. Grosset, K. W. Broman, and W. R. Bishai.** 2003. A postgenomic method for predicting essential genes at subsaturation levels of mutagenesis: application to *Mycobacterium tuberculosis*. Proc. Natl. Acad. Sci. USA **100:**7213–7218.
19. **Larocque, R. C., J. B. Harris, M. Dziejman, X. Li, A. I. Khan, A. S. Faruque, S. M. Faruque, G. B. Nair, E. T. Ryan, F. Qadri, J. J. Mekalanos, and S. B. Calderwood.** 2005. Transcriptional profiling of *Vibrio cholerae* recovered directly from patient specimens during early and late stages of human infection. Infect. Immun. **73:**4488–4493.
20. **Li, L., J. P. Bannantine, Q. Zhang, A. Amonsin, B. J. May, D. Alt, N. Banerji, S. Kanjilal, and V. Kapur.** 2005. The complete genome sequence of *Mycobacterium avium* subspecies *paratuberculosis*. Proc. Natl. Acad. Sci. USA **102:**12344–12349.
21. **Linnabary, R. D., G. L. Meerdink, M. T. Collins, J. R. Stabel, R. W. Sweeney, M. K. Washington, and S. J. Wells.** 2001. Johne's disease in cattle. Counc. Agric. Sci. Technol. **17:**1–10.
22. **Manganelli, R., E. Dubnau, S. Tyagi, F. R. Kramer, and I. Smith.** 1999. Differential expression of 10 sigma factor genes in *Mycobacterium tuberculosis*. Mol. Microbiol. **31:**715–724.
23. **Manganelli, R., R. Prov1, S. Rodrigue, J. Beaucher, L. Gaudreau, and I. Smith.** 2004. Sigma factors and global gene regulation in *Mycobacterium tuberculosis*. J. Bacteriol. **186:**895–902.
24. **Manganelli, R., M. I. Voskuil, G. K. Schoolnik, E. Dubnau, M. Gomez, and I. Smith.** 2002. Role of the extracytoplasmic-function sigma factor sigma(H) in *Mycobacterium tuberculosis* global gene expression. Mol. Microbiol. **45:**365–374.
25. **McKinney, J. D., K. Höner zu Bentrup, E. J. Muñoz-Elias, A. Miczak, B. Chen, W. T. Chan, D. Swenson, J. C. Sacchettini, W. R. Jacobs, Jr., and D. G. Russell.** 2000. Persistence of *Mycobacterium tuberculosis* in macrophages and mice requires the glyoxylate shunt enzyme isocitrate lyase. Nature **406:**735–738.
26. **Momotani, E., D. L. Whipple, A. B. Thiermann, and N. F. Cheville.** 1988. Role of M cells and macrophages in the entrance of *Mycobacterium paratuberculosis* into domes of ileal Peyer's patches in calves. Vet. Pathol. **25:**131–137.
27. **Naser, S. A., G. Ghobrial, C. Romero, and J. F. Valentine.** 2004. Culture of Mycobacterium avium subspecies paratuberculosis from the blood of patients with Crohn's disease. Lancet **364:**1039–1044.
28. **Naser, S. A., I. Shafran, D. Schwartz, F. El Zaatari, and J. Biggerstaff.** 2002. In situ identification of mycobacteria in Crohn's disease patient tissue using confocal scanning laser microscopy. Mol. Cell. Probes **16:**41–48.
29. **Paustian, M. L., A. Amonsin, V. Kapur, and J. P. Bannantine.** 2004. Characterization of novel coding sequences specific to *Mycobacterium avium* subsp. *paratuberculosis*: implications for diagnosis of Johne's disease. J. Clin. Microbiol. **42:**2675–2681.
30. **Petersohn, A., M. Brigulla, S. Haas, J. D. Hoheisel, U. Volker, and M. Hecker.** 2001. Global analysis of the general stress response of *Bacillus subtilis*. J. Bacteriol. **183:**5617–5631.
31. **Phillips, B. J., and W. Kaplan.** 1976. Effect of cetylpyridinium chloride on pathogenic fungi and *Nocardia asteroides* in sputum. J. Clin. Microbiol. **3:**272–276.

32. **Raman, S., T. S. Song, X. L. Puyang, S. Bardarov, W. R. Jacobs, and R. N. Husson.** 2001. The alternative sigma factor SigH regulates major components of oxidative and heat stress responses in *Mycobacterium tuberculosis*. J. Bacteriol. **183:**6119–6125.

33. **Sassetti, C. M., and E. J. Rubin.** 2003. Genetic requirements for mycobacterial survival during infection. Proc. Natl. Acad. Sci. USA **100:**12989–12994.

34. **Schnappinger, D., S. Ehrt, M. I. Voskuil, Y. Liu, J. A. Mangan, I. M. Monahan, G. Dolganov, B. Efron, P. D. Butcher, C. Nathan, and G. K. Schoolnik.** 2003. Transcriptional adaptation of *Mycobacterium tuberculosis* within macrophages: insights into the phagosomal environment. J. Exp. Med. **198:**693–704.

35. **Semret, M., D. C. Alexander, C. Y. Turenne, P. de Haas, P. Overduin, D. van Soolingen, D. Cousins, and M. A. Behr.** 2005. Genomic polymorphisms for *Mycobacterium avium* subsp. *paratuberculosis* diagnostics. J. Clin. Microbiol. **43:**3704–3712.

36. **Shin, S. J., C.-W. Wu, H. Steinberg, and A. M. Talaat.** 2006. Identification of novel virulence determinants in *Mycobacterium paratuberculosis* by screening a library of insertional mutants. Infect. Immun. **7:**3825–3833.

37. **Singh-Gasson, S., R. D. Green, Y. J. Yue, C. Nelson, F. Blattner, M. R. Sussman, and F. Cerrina.** 1999. Maskless fabrication of light-directed oligonucleotide microarrays using a digital micromirror array. Nat. Biotechnol. **17:**974–978.

38. **Souza, C. D., O. A. Evanson, and D. J. Weiss.** 2006. Mitogen activated protein kinase p38 pathway is an important component of the anti-inflammatory response in *Mycobacterium avium* subsp. *paratuberculosis*-infected bovine monocytes. Microb. Pathog. **41:**59–66.

39. **Springer, B., S. Master, P. Sander, T. Zahrt, M. McFalone, J. Song, K. G. Papavinasasundaram, M. J. Colston, E. Boettger, and V. Deretic.** 2001. Silencing of oxidative stress response in *Mycobacterium tuberculosis*: expression patterns of *ahpC* in virulent and avirulent strains and effect of *ahpC* inactivation. Infect. Immun. **69:**5967–5973.

40. **Stermann, M., L. Sedlacek, S. Maass, and F. C. Bange.** 2004. A promoter mutation causes differential nitrate reductase activity of *Mycobacterium tuberculosis* and *Mycobacterium bovis*. J. Bacteriol. **186:**2856–2861.

41. **Stewart, D. J., J. A. Vaughan, P. L. Stiles, P. J. Noske, M. L. V. Tizard, S. J. Prowse, W. P. Michalski, K. L. Butler, and S. L. Jones.** 2006. A long-term study in Angora goats experimentally infected with Mycobacterium avium subsp paratuberculosis: clinical disease, faecal culture and immunological studies. Vet. Microbiol. **113:**13–24.

42. **Stewart, G. R., B. D. Robertson, and D. B. Young.** 2004. Analysis of the function of mycobacterial DnaJ proteins by overexpression and microarray profiling. Tuberculosis **84:**180–187.

43. **Stewart, G. R., L. Wernisch, R. Stabler, J. A. Mangan, J. Hinds, K. G. Laing, D. B. Young, and P. D. Butcher.** 2002. Dissection of the heat-shock response in Myobacterium tuberculosis using mutants and microarrays. Microbiology **148:**3129–3138.

44. **Talaat, A. M., S. T. Howard, I. W. Hale, R. Lyons, H. Garner, and S. A. Johnston.** 2002. Genomic DNA standards for gene expression profiling in *Mycobacterium tuberculosis*. Nucleic Acids Res. **30:**E104.

45. **Talaat, A. M., P. Hunter, and S. A. Johnston.** 2000. Genome-directed primers for selective labeling of bacterial transcripts for DNA microarray analysis. Nat. Biotechnol. **18:**679–682.

46. **Talaat, A. M., R. Lyons, S. T. Howard, and S. A. Johnston.** 2004. The temporal expression profile of *Mycobacterium tuberculosis* infection in mice. Proc. Natl. Acad. Sci. USA **101:**4602–4607.

47. **Talaat, A. M., and M. Trucksis.** 2000. Transformation and transposition of the genome of *Mycobacterium marinum*. Am. J. Vet. Res. **61:**125–128.

48. **Talaat, A. M., S. K. Ward, C.-W. Wu, E. Rondon, C. Tavano, J. P. Bannantine, R. Lyons, and S. A. Johnston.** 2007. Mycobacterial bacilli are metabolically active during chronic tuberculosis in murine lungs: insights from genome-wide transcriptional profiling. J. Bacteriol. **189:**4265–4274.

49. **Tooker, B. C., J. L. Burton, and P. M. Coussens.** 2002. Survival tactics of *M. paratuberculosis* in bovine macrophage cells. Vet. Immun. Immunopathol. **87:**429–437.

50. **Voskuil, M. I., D. Schnappinger, K. C. Visconti, M. I. Harrell, G. M. Dolganov, D. R. Sherman, and G. K. Schoolnik.** 2003. Inhibition of respiration by nitric oxide induces a *Mycobacterium tuberculosis* dormancy program. J. Exp. Med. **198:**705–713.

51. **Whittington, R. J., and E. S. G. Sergeant.** 2001. Progress towards understanding the spread, detection and control of *Mycobacterium avium* subsp. *paratuberculosis* in animal populations. Aust. Vet. J. **79:**267–278.

52. **Wu, C.-W., J. Glasner, M. T. Collins, S. Naser, and A. M. Talaat.** 2006. Whole-genome plasticity among *Mycobacterium avium* subspecies: insights from comparative genomic hybridizations. J. Bacteriol. **188:**711–723.

53. **Wu, C. W., M. Livesey, S. K. Schmoller, E. J. B. Manning, H. Steinberg, W. C. Davis, M. J. Hamilton, and A. M. Talaat.** 2007. Invasion and persistence of *Mycobacterium paratuberculosis* during early stages of Johne's disease in calves. Infect. Immun. **75:**2110–2119.

54. **Zaslaver, A., A. E. Mayo, R. Rosenberg, P. Bashkin, H. Sberro, M. Tsalyuk, M. G. Surette, and U. Alon.** 2004. Just-in-time transcription program in metabolic pathways. Nat. Genet. **36:**486–491.